Fast relaxation intensity versus silica glass density: existence of sharp peculiarity

2006 J. Phys.: Condens. Matter 18 4763

(http://iopscience.iop.org/0953-8984/18/19/027)

INSTITUTE OF PHYSICS PUBLISHING JOURNAL OF PHYSICS: CONDENSED MATTER

J. Phys.: Condens. Matter **18** (2006) 4763–4771 doi:10.1088/0953-8984/18/19/027

Fast relaxation intensity versus silica glass density: existence of sharp peculiarity

N V Surovtsev[1], S V Adichtchev[1], V K Malinovsky[1], A A Kalinin[2] and Yu N Pal'yanov[2]

[1] Institute of Automation and Electrometry, Russian Academy of Sciences, Novosibirsk 630090, Russia
[2] United Institute of Geology, Geophysics, and Mineralogy, Russian Academy of Sciences, Novosibirsk 630090, Russia

Received 1 March 2006
Published 27 April 2006
Online at stacks.iop.org/JPhysCM/18/4763

Abstract

Low-frequency Raman spectra of densified silica glasses, annealed at different temperatures and possessing various densities, are studied. The dependence of the fast relaxation intensity versus the density can be described by linear laws below and above the density 2.26 g cm^{-3}, but the slope of the linear law below the critical density is ten times higher than the slope of the linear law above 2.26 g cm^{-3}. The sharp peculiarity is interpreted as a consequence of an inhomogeneous glassy structure with local ordering similar to tridimite or β-cristobalite. The dependence of the silica sample density on annealing temperature is discussed in view of the temperature dependence of the liquid silica density. A hypothesis is proposed that the true dependence of the liquid silica density is a linear function of temperature.

1. Introduction

The ability of glassy silica to change its density significantly after pressure treatment [1] is very attractive, since it allows researchers to study a glass with the same chemical composition, at the same pressure–temperature parameters, but in different morphic states. Densified silica glasses have minor changes in short-range structural order and, therefore, the densification effects are related to some changes in the nanometre-scale structure. That is why the medium-range order, boson peak and fast relaxation spectrum are actively studied in densified silica. In particular, Raman [2], neutron [3], inelastic x-ray scattering [4–6], specific heat [7] data, and molecular dynamics simulation results [8, 9] are now available for the boson peak in densified silica. In our recent research, it was found that the densification of silica not only suppresses the low-energy part of the boson peak and of the Raman coupling coefficient, but also strongly suppresses the intensity of fast relaxation [10]. In this work, experimental low-frequency Raman spectra were described using the model of a damped oscillator [11–14]. Within this

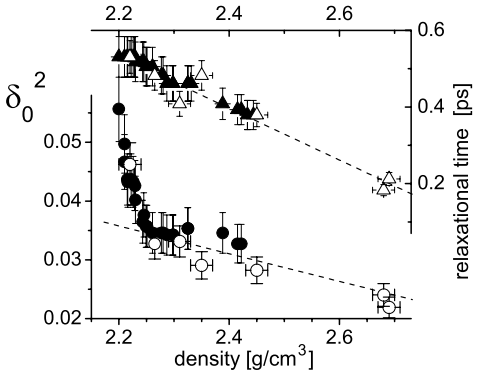

Figure 1. Parameters of the fast relaxational spectrum versus the sample density: δ_0^2 (circles, left axis) and relaxational time (triangles, right axis). The open symbols correspond to data from [10] and the close symbols to the present work. The lines are guides for eyes.

model, the fast relaxation is manifested in the light scattering spectra as a relaxational part of the response of boson peak vibrations, and the whole spectrum is written as [14]

$$I_n(T,\nu) = \frac{2}{\pi}\int_0^\infty \frac{I_n^v(T,\Omega)\Omega^4\delta_0^2\gamma/(\nu^2+\gamma^2)\,\mathrm{d}\Omega}{(\Omega^2-\nu^2-\delta_0^2\gamma^2\Omega^2/(\nu^2+\gamma^2))^2+(\delta_0^2\gamma\Omega^2\nu/(\nu^2+\gamma^2))^2}, \tag{1}$$

where $I_n(\nu) = I(\nu)/[(n+1)\nu]$ is the Raman spectrum in the spectral density presentation (here, n is the Bose factor), I_n^v is the vibrational spectrum, γ is the width of the relaxational spectrum related to the relaxational time τ via $\gamma = 1/(2\pi\tau)$, and δ_0^2 is the damping parameter, which is proportional to the integral over the relaxational part of the spectrum [14]. In [10], it was found that the parameter δ_0^2, reflecting the fast relaxation intensity, has an unexpected dependence as a function of the sample density ρ. A relatively moderate increase in δ_0^2 as ρ decreases from 2.68 to 2.26 g cm^{-3} is changed by outstanding δ_0^2 for the ρ of normal silica glass (data from [10] are shown in figure 1 by open symbols). A residuary question is, how sharp is this transition?

Work presented here was devoted to this topic. Since the direct high-pressure synthesis of silica glasses with various densities in a narrow density range $\rho = 2.2$–2.3 g cm^{-3} is a cumbersome method, an alternative approach was chosen, where a densified silica sample was annealed down to the desired density. The practicability of this method relates to a property of the densified silica glass to reduce its density during annealing at high temperatures [15]. Analysis of experimental Raman spectra of silica samples with different densities allowed us to demonstrate unequivocally the existence of a sharp peculiarity at $\rho = 2.26$ g cm^{-3} for the fast relaxation intensity. The dependence of the relaxed silica density versus the annealing temperature, obtained in our study, turns us to a discussion of the topic—what is the temperature dependence of the equilibrium silica density? We question Bruckner's interpretation of $\rho(T)$ [16] and suggest a linear $\rho(T)$ dependence.

2. Experimental details

The preparation of silica samples with a smoothly varying density included an initial densification under high-pressure–temperature conditions, followed by annealing at a fixed temperature. In [15], it was shown that, at the given temperature, the density relaxes most significantly in the first 10 min and then much more slowly in the temporary range >1 h. The initial quick decrease in the density depends strongly on the annealing temperature. Thus,

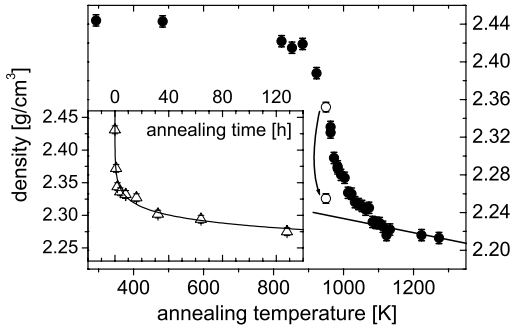

Figure 2. Sample density after 1 h anneal versus annealing temperature. The line is the high-temperature description by equation (3). Using open circles, the sample density after 1 and 128 h of annealing at $T = 950$ K is added. The inset shows the annealing time dependence of a densified silica sample during annealing at $T = 950$ K. The line is fitted by equation (4).

the optimal procedure for achieving different densities is the annealing of densfied silica for ∼1 h at different temperatures. The higher the annealing temperature, the lower the relaxed density [15].

Densified silica samples with a density of ∼2.45 g cm^{-3} were produced from type I silica [16] by the application of high-temperature, high-pressure conditions ($P = 50$ kbar, $T = 820$ K, 20 h) to silica cylinders of a height and diameter of 4 mm, as described in [10]. Further sample treatment was annealing for 1 h at different temperatures in the range 480–1270 K (from low temperature to high temperature). After each annealing temperature, the sample density and Raman scattering spectrum were measured at ambient conditions. The sample density was found by weighing in distilled water with a precision of ∼0.005 g cm^{-3}. Also, a study of the kinetics of the density change during prolonged annealing at $T = 950$ K was undertaken.

Depolarized (HH) Raman right-angle experiments were performed using the 532 nm line from a solid-state laser with a power of 800 mW, and a triple spectrograph TriVista 777 from S&I/PiActon. Raman spectra were recorded in a multichannel regime using a silicon CCD matrix with a spectral resolution of ∼1 cm^{-1}.

3. Results and discussion

3.1. Raman spectra

The sample density after annealing for 1 h versus annealing temperature T_{an} is shown in figure 2. After annealing at $T_{an} > 800$ K, the sample density decreases. As is seen (figure 2), there is the possibility of obtaining quite accurately any density in the range 2.45–2.22 g cm^{-3}. Depolarized Raman spectra of silica samples were measured (representative spectra can be found in the previous publication [10]) and fitted by the expression (1). The parameters of the fast relaxational spectrum are shown in figure 1 versus the sample density using the solid symbols. It is seen that, while there are no significant peculiarities in $\tau(\rho)$, the fast relaxation intensity, parameter δ_0^2, undergoes a sharp-ish change in its behaviour near $\rho = 2.26$ g cm^{-3}. To a rough approximation, the $\delta_0^2(\rho)$ dependence can be described by two linear laws above and below $\rho = 2.26$ g cm^{-3}, and their slopes differ by more than ten times!

It seems to be important to demonstrate that the sharp transition near $\rho = 2.26$ g cm^{-3} is not a specificity of fitting by equation (1), but reflects the internal changes of the low-frequency

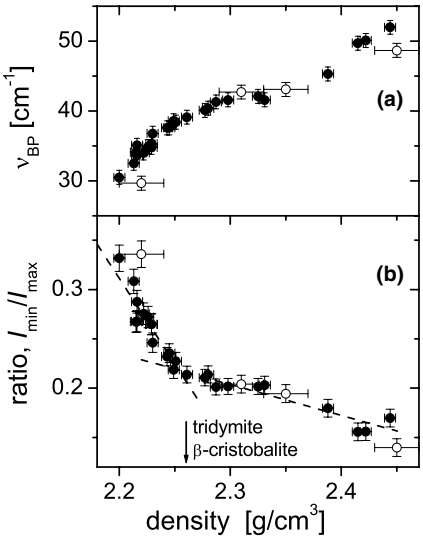

Figure 3. Apparent characteristics of low-frequency spectrum versus the sample density. The open symbols correspond to data from [10]; the closed symbols to the present work. (a) Boson peak position, ν_{BP}. (b) Ratio of low-frequency minimum and maximum intensities. The lines are linear fits below and above $\rho = 2.26$ g cm^{-3}.

Raman spectra. For this reason, the apparent characteristics of the Raman spectra, measured in the present and previous [10] works, were plotted versus the sample density. In figure 3(a), the position of the boson peak maximum, ν_{BP}, is presented. ν_{BP} was defined from a spectral presentation

$$\frac{I(\nu)}{(n+1)\nu^2}, \tag{2}$$

which is proportional to the density of states divided by the squared frequency, $g(\nu)/\nu^2$, in the approximation that the Raman coupling coefficient is proportional to the frequency (the coupling coefficient of densified silica is discussed in [10] in more detail). $\nu_{BP}(\rho)$ has no sharp peculiarity near $\rho = 2.26$ g cm^{-3} (figure 3(a)). The experimental $\nu_{BP}(\rho)$ corresponds rather to a gradual modification of the vibrational spectrum as the density changes. A relative contribution of the fast relaxation spectrum to the whole spectrum can be estimated from the ratio I_{min}/I_{max} between the intensities of the spectral minimum near 10 cm^{-1}, where the relaxational spectrum dominates, and the spectral maximum, where the vibrational spectrum dominates (an example of such an analysis is [17]). Thus, this ratio somehow reflects the relative contribution of the fast relaxation spectrum. The ratio I_{min}/I_{max} is shown in figure 3(b). A sharp peculiarity near $\rho = 2.26$ g cm^{-3} for the density dependence of this ratio is clearly seen. Slopes of linear fits below and above $\rho = 2.26$ g cm^{-3} differ by 5.5 times.

The strong suppression of the fast relaxation contribution to Raman spectra of the silica samples with $\rho > 2.26$ g cm^{-3} can be discussed from a viewpoint that implies description of the silica dynamics in terms of rigid unit modes (RUMs) [18, 19]. RUMs are modes that do not involve the distortion of SiO_4 tetrahedra. These modes correspond to the vibration or relaxation response at low frequencies, which have rather large amplitudes. Different intensities of the fast relaxational spectrum for different silica samples are attributed to the change in the ability of glass structures to support RUMs. From figures 1 and 3, one can conclude that silica samples with $\rho < 2.26$ g cm^{-3} can support RUMs, i.e. they are 'floppy', whereas samples

with $\rho > 2.26$ g cm^{-3} are 'stiff' and do not have RUMs (or have a small amount). The existence of an RUM is related to relatively weak topological constraints for a tetrahedron, implying flexibility of the structure against floppy modes [18, 20]. The suppression of RUMs corresponds to a glassy structure with only stiff tetrahedra. The question is, what is it about the density of 2.26 g cm^{-3} that makes the silica change its low-frequency dynamics so drastically?

The critical value $\rho = 2.26$ g cm^{-3} is equal to those of the low-density crystalline SiO_2 polymorphs, tridymite and β-cristobalite. The sharp peculiarity in $\delta_0^2(\rho)$ can be interpreted as a consequence of an inhomogeneous glassy structure [10]. In the framework of this interpretation, in typical silica glass the local packing of SiO_4 tetrahedra has favourable structures such as β-cristobalite (or tridimite), providing nanoclusters, and more disordered, less dense regions, which play the role of relaxation centres (or, in other words, are sources of RUMs). In the models that exploit the inhomogeneous structure of glasses [21–23], the boson peak is interpreted as vibrational modes relating to nanoclusters. It is often accepted that less dense regions (sometimes the term 'free volume' is used) cause the high anharmonicity in glassy dynamics [14], resulting in the relaxational dynamical response. There are works where an interrelation between silica and low-density crystalline SiO_2 polymorphs is suggested; for example, [24–26]. We believe that a 'weak' densification with $\rho < 2.26$ g cm^{-3} is mainly related to the decrease in the number of weak, highly disordered regions, therefore resulting in the significant decrease in the fast relaxation intensity. From this viewpoint, the density 2.26 g cm^{-3} corresponds to a minimum in the concentration of weak, less dense regions for the given local packing of SiO_4 tetrahedra. Densification to densities higher than 2.26 g cm^{-3} is related mainly to a change in the type of local favourable ordering, with the fast relaxation intensity slowly decreasing as the density increases. Thus, our finding supports the viewpoint that there is a tendency of the local structure of normal silica glass to take on an ordering similar to the low-density crystalline SiO_2 polymorphs. But the sharpness of this transition (figures 1 and 3(b)) is outstanding. The sharpness is interpreted as a consequence of the large difference in compressibility of the nanoclusters and the less dense regions.

There exists an interpretation of the relaxational processes in silica for the range above 30 GHz [27, 28], assuming the domination of the anharmonic coupling of acoustic vibrations by thermally excited modes (so-called 'network viscosity'). The difference in internal friction at the Brillouin frequency for densified ($\rho = 2.63$ g cm^{-3}) and normal silica, which appears to be five times smaller than for densified glass (at $T = 300$ K), in [28] was interpreted as a consequence of the shorter mean lifetime τ_{th} of the thermal modes in the densified silica. In turn, the smaller value of τ_{th} in densified silica was considered in [28] to be a reflection of a higher value of the crossover frequency ν_{co}, beyond which the acoustic excitations become diffusive. According to [29] the boson peak position ν_{BP} is a rather accurate estimate for ν_{co}. Thus, in the framework of the model of [28], a correlation between the increase in ν_{BP} and the decrease in the fast relaxation intensity in densified silica should be observed. However, this is not the case (figure 3). This means that the simple model of [28] should be developed further.

3.2. Silica density versus temperature

As is seen in figure 2, the dependence of the relaxed density on annealing temperature (after 1 h of treatment) includes three regions: the first, below 900 K, where the density change is small or absent; the interval 900–1000 K, with a strong dependence of the annealed density on T_{an}; and at $T_{an} > 1000$ K. We believe that the third region corresponds to a regime where one gets a silica glass, close to equilibrium liquid silica at a given temperature. Indeed, in the production of typical glass, its density and other physical parameters reflect somewhat the liquid (equillibrium) state at the glass transition temperature, T_g (for silica glass, $T_g = 1450$ K [30]).

The abrupt increase in the primary relaxation time prevents production of glasses with a structure corresponding to equilibrium silica at a temperature significantly lower than T_g. Thus, in the normal case, the glass density is lower than a linear extrapolation of the temperature dependence from the liquid state (figures 2.1, 2.2 in [30]). Annealing of the silica glass, starting from a state denser than liquid silica at a given temperature, gives us the possibility of achieving a state which is not inaccessible in normal cooling through the glass transition. If this is true, one should expect that the recovered density ρ_∞ at significantly long annealing time is equal to the equilibrium liquid silica density ρ_L at $T = T_{an}$. It is expected (for example, figures 2.1, 2.2 in [30]) that $\rho_L(T)$ is a more or less linear function of T, being equal to the density of normal silica glass ($\rho_0 = 2.20$ g cm^{-3}) at $T = T_g$. Therefore, one could expect the validity of the expression

$$\rho_\infty(T_{an}) = \rho_0 + \alpha(T - T_g), \tag{3}$$

where α is a coefficient. The linear fit by expression (3) is shown in figure 2 for the high-temperature part, where the time for complete density relaxation is expected to be shorter. This line goes reasonably well through experimental points at $T_{an} > 1080$ K ($\alpha = 7.5 \times 10^{-5}$ g cm^{-3} K^{-1}).

In the spirit of the interpretation of $\rho_\infty(T_{an})$, it is expected that the deviation from expression (3) at $T_{an} < 1080$ K is related to not enough annealing time in order to achieve the equilibrium ρ_∞. In order to inspect this hypothesis, the density dependence on the annealing time τ_{an} was studied at $T_{an} = 950$ K. Results are shown in the inset of figure 2. It is seen that, while the density change is much slower at $\tau_{an} > 1$ h, nevertheless it can provide a significant contribution to the final ρ_∞. In figure 2, it is seen that, after annealing for 128 h, the resulting density is close to the density, predicted by the fit of expression (3). This result supports our hypothesis about the relation between the state of densified silica glasses after annealing and the equilibrium glassy silica state. The present interpretation is in the spirit of [31], where a state of amorphized zeolites was described as a state that is non-achievable by simple cooling due to kinetic limitations.

In the inset of figure 2, the time dependence is described by logarithmic relaxation:

$$\rho(\tau_{an}) \propto A - \log(\tau_{an}). \tag{4}$$

This description works quite well. The logarithmic law was reported before for the time-dependent density changes of irradiated silica [32], the density changes during silica densification at $P = 9$ GPa [33], and the Brillouin frequency shift of densified silica at $T \leqslant 673$ K [34]. Our finding is in line with these works. But, surely, the logarithmic law is only an approximation for intermediate τ_{an} and, for a sufficiently long annealing time, the exponential or stretched exponential laws are more adequate. Indeed, the density relaxation at higher annealing temperature shows the deviation from logarithmic law clearly [35].

Let us consider the hypothesis that the state of densified silica glass after annealing at T_{an}, equivalent to the equilibrium silica at T_{an}, would be provided by cooling. In this case, $\rho_\infty(T_{an})$ should be compared with $\rho(T)$ of the liquid silica. In figure 4, the molecular volume of densified glasses after the annealing treatment is shown versus the annealing temperature, together with the liquid silica data of [36] (this is the only direct density data of liquid silica that we were able to find). Also, a point for typical silica glass $\rho(T_g)$ is shown. The solid line is our version of the equilibrium $\rho(T)$ dependence, extrapolating the linear equation (3) to $T > T_g$ range. This extrapolation corresponds to the text-book linear approximation for the temperature dependence of the molecular volume, which works quite well in most glass-formers [30]. The extrapolation agrees with the data of [36] only on a qualitative level, and disagrees by 3% in absolute values with the four lowest data points and by 9% for highest temperature of [36].

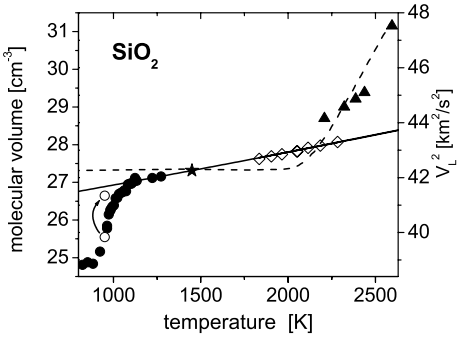

Figure 4. Molecular volume of silica versus temperature. The triangles are for liquid silica; data from [36]. The circles are annealing (after 1 h) data from the present work. The star is the point for normal glass versus the glass transition temperature. The open circles are the same as in figure 2. The dashed line is $V_m(T)$, as described by Brückner [16], and the solid line is $V_m(T)$, corresponding to equation (3). The diamonds are squared longitudinal sound velocities of liquid silica (right axis) versus temperature; data from [38].

The widely used Bruckner's interpretation of $\rho(T)$ [16] is in contradiction with ours. Bruckner's interpretation, shown in figure 4 by the dashed line, is based on the results of room-temperature density of silica samples with different fictive temperatures and density data of [36]. Bruckner's $\rho(T)$ includes a density maximum near 1770 K (the corresponding molecular volume minimum is too fine to be seen well in the present figure). However, recently Shelby [37] questioned this result; according to his work, the density maximum does not occur for fictive temperatures below 1900 K. In [37], the fictive temperatures were determined by the characteristics of the infrared absorption band instead of the heat treatment temperature in [16]. Moreover, we believe that the problem of matching a heat-treated silica glass to a temperature, where the equilibrium liquid state of silica is the same, is not solved.

According to Bruckner's $\rho(T)$, there is a sharp peculiarity of $\rho(T)$ in the liquid state of silica, occurring near 2000 K. In this case, one should expect the existence of a peculiarity for other characteristics of liquid silica. There are Brillouin data for liquid silica in the range $T = 1835$–2283 K [38]. The squared longitudinal sound velocity, V_L^2, is determined by the ratio

$$V_L^2 = C_{11}/\rho \tag{5}$$

where C_{11} is the longitudinal modulus. V_L^2 versus temperature from [38] is shown in figure 4. It is seen that $V_L^2(T)$ is quasilinear and has no sharp peculiarities expected from Bruckner's $\rho(T)$. Thus, Brillouin data does not support Bruckner's $\rho(T)$. In contrast, the quasilinear behaviour of $V_L^2(T)$ is well accounted for by a linear $\rho(T)$. In the approximation $C_{11}(T) \approx$ const, the squared longitudinal sound velocity is proportional to the molecular volume. According to [38], $V_L^2(T)$ increases by 1.4% in the range $T = 1835$–2283 K. The linear dependence shown in figure 4 corresponds to an increase in the molecular volume V_m by 1.5% in the range $T = 1835$–2283 K. This agreement supports the linear behaviour for $\rho(T)$ over the whole temperature range.

Surely, the assumed temperature independence of the longitudinal elastic modulus can be questioned. In order to fit simultaneously the density data of [36] and the $V_L^2(T)$ of [38], C_{11} should decrease by ~3% as the temperature increases in the range $T = 1835$–2283 K. However, for the monocomponent strong network glass formers studied (B_2O_3, GeO_2), the longitudinal elastic modulus is either temperature independent or weakly increases with increasing temperature far above the glass transition [39, 40]. Also, Brillouin data below T_g

in SiO_2 demonstrate that C_{11} increases [38, 39]. Thus, it is reasonably to expect that, in liquid silica, C_{11} is either temperature independent or weakly increases with increasing temperature, making it impossible to fit simultaneously the $\rho(T)$ of [36] and the $V_L^2(T)$ of [38]. Thus, there is a necessity to inspect the $\rho(T)$ of silica liquid more precisely.

The last statement reflects our worries about the precision of the liquid silica density, found in [36] (the precision of ρ is not indicated in this work). There are a few points in this work to which the attention should be paid: the assumption of the temperature independence for the surface tension of liquid silica and the disagreement between the rising and descending sphere slopes. For example, the rising and descending slopes differ by ∼20% (figure 6 of [36]), which was explained by the influence of the silica adhering to the rod. Independent linear fits for the digitized data of this figure produce about ∼1% difference for the weights of the tungsten sphere in the liquid silica W_g, for the rising and descending spheres. If a value of 1% is taken, in a rough approximation, as the precision of W_g, then a level of ∼10% precision is expected for the silica density (tungsten is about ten times denser than silica) for the data of [36]. It is seen from figure 4 that this precision covers the difference between the extrapolation of $\rho(T)$ by equation (3) and the data of [36]. More accurate measurements of liquid silica density are needed in order to clarify this point.

4. Conclusion

To conclude, the low-frequency Raman spectra of silica glasses with various densities, prepared by annealing of pressure densified samples at different temperatures, were studied. A sharp peculiarity at $\rho = 2.26$ g cm^{-3} was found for the fast relaxation dependence on the silica glass density. The density 2.26 g cm^{-3} corresponds to the low-density crystalline SiO_2 polymorphs, β-cristobalite and tridimite. The finding was interpreted as a manifestation of inhomogeneous silica glass structure, consisting of nanometre-scale clusters with cristobalite-like (or tridimite-like) local ordering and less dense, weak regions, which are responsible for the fast relaxation intensity and have compressibility lower than that of nanoclusters.

The state of silica samples, fully relaxed at the annealing temperature T_{an}, is interpreted as the analogue of the equilibrium state at the given T_{an}. Within this interpretation, an analysis of the sample density versus annealing temperature provides a linear description for the temperature dependence of the equilibrium silica density, $\rho(T)$. Extrapolation of the linear $\rho(T)$ to the temperature range above the glass transition is in an excellent agreement with Brillouin data [38], if the temperature dependence of compressibility is considered to be negligible. But the proposed linear $\rho(T)$ contradicts Bruckner's interpretation of $\rho(T)$, which is widely used, and in poor agreement with the direct measurements of [36]. Further *in situ* experimental studies of silica density in the temperature range above the glass transition are needed in order to clarify this point.

Acknowledgment

This work was supported by the Interdisciplinary Science Fund at the Russian Foundation for Basic Research of the Siberian Branch of the Russian Academy of Sciences (project No. 140).

References

[1] Bridgman P W and Simon I 1953 *J. Appl. Phys.* **24** 405
[2] Sugai S and Onodera A 1996 *Phys. Rev. Lett.* **77** 4210

[3] Inamura Y, Arai M, Nakamura M, Otomo T, Kitamura N, Bennington S M, Hannon A C and Buchenau U 2001 *J. Non-Cryst. Solids* **293–295** 389
[4] Rat E, Foret M, Courtens E, Vacher R and Arai M 1999 *Phys. Rev. Lett.* **83** 1355
[5] Foret M, Vacher R, Courtens E and Monaco G 2002 *Phys. Rev.* B **66** 024204
[6] Rufflé B, Foret M, Courtens E, Vacher R and Monaco G 2003 *Phys. Rev. Lett.* **90** 095502
[7] Liu X, Löhneysen H v, Weiss G and Arndt J 1995 *Z. Phys.* B **99** 49
[8] Pilla O, Angelani L, Fontana A, Gonçalves J R and Ruocco G 2003 *J. Phys.: Condens. Matter* **15** S995
[9] Trachenko K and Dove M T 2003 *Phys. Rev.* B **67** 064107
[10] Surovtsev N V, Malinovsky V K, Pal'yanov Yu N, Kalinin A A and Shebanin A P 2004 *J. Phys.: Condens. Matter* **16** 3035
[11] Winterling G 1975 *Phys. Rev.* B **12** 2432
[12] Gochiyaev V Z, Malinovsky V K, Novikov V N and Sokolov A P 1991 *Phil. Mag.* B **63** 777
[13] Sokolov A P, Novikov V N and Strube B 1997 *Europhys. Lett.* **38** 49
[14] Novikov V N, Sokolov A P, Strube B, Surovtsev N V, Duval E and Mermet A 1997 *J. Chem. Phys.* **107** 1057
[15] Mackenzie J D 1963 *J. Am. Ceram. Soc.* **46** 10
[16] Brückner R 1970 *J. Non-Cryst. Solids* **5** 123
[17] Sokolov A P, Rössler E, Kisliuk A and Quitmann D 1993 *Phys. Rev. Lett.* **71** 2062
[18] Trachenko K and Dove M T 2002 *J. Phys.: Condens. Matter* **14** 1143
[19] Trachenko K, Dove M T, Brazhkin V and El'kin F S 2004 *Phys. Rev. Lett.* **93** 135502
[20] Trachenko K, Dove M T, Harris M and Heine V 2000 *J. Phys.: Condens. Matter* **12** 8041
[21] Duval E, Bourkenter A and Achibat T 1990 *J. Phys.: Condens. Matter* **2** 10227
[22] Sokolov A P, Kisliuk A, Soltwisch M and Quitmann D 1992 *Phys. Rev. Lett.* **69** 1540
[23] Surovtsev N V 2004 *Phys. Status Solidi* c **11** 2867
[24] Dove M T, Harris M J, Hannon A C, Parker J M, Swainson I P and Gambhir M 1997 *Phys. Rev. Lett.* **78** 1070
[25] Nakamura M, Arai M, Otomo T, Inamura Y and Bennington S M 2001 *J. Non-Cryst. Solids* **293–295** 377
[26] Nakamura M, Arai M, Inamura Y, Otomo T and Bennington S M 2003 *Phys. Rev.* B **67** 064204
[27] Rat E, Foret M, Massiera G, Vialla R, Arai M, Vacher R and Courtens E 2005 *Phys. Rev.* B **72** 214204
[28] Vacher R, Courtens E and Foret M 2005 *Phys. Rev.* B **72** 214205
[29] Rufflé B, Guimbretière G, Courtens E, Vacher R and Monaco G 2006 *Phys. Rev. Lett.* **96** 045502
[30] Elliott S R 1990 *Physics of Amorphous Materials* (London: Longman Scientific&Technical)
[31] Greaves G N, Meneau F, Sapelkin A, Colyer L M, Gwynn I A, Wade S and Sankar G 2003 *Nat. Mater.* **2** 622
[32] Primak W and Szymanski H 1956 *Phys. Rev.* **101** 1268
[33] Tsiok O B, Brazhkin V V, Lyapin A G and Khvostantsev L G 1998 *Phys. Rev. Lett.* **80** 999
[34] Karpov V G and Grimsditch M 1993 *Phys. Rev.* B **48** 6941
[35] Höfler S and Seifert F 1984 *Earth Planet. Sci. Lett.* **67** 433
[36] Bacon J F, Hasapis A A and Wholley J W 1960 *Phys. Chem. Glasses* **1** 90
[37] Shelby J E 2004 *J. Non-Cryst. Solids* **349** 331
[38] Polian A, Vo-Thanh D and Richet P 2002 *Europhys. Lett.* **57** 375
[39] Kieffer J 1994 *Phys. Rev.* B **50** 17
[40] Youngman R E, Kieffer J, Bass J D and Duffrene L 1997 *J. Non-Cryst. Solids* **222** 190